



Published in final edited form as:

FEBS Lett. 2016 September ; 590(17): 2844–2851. doi:10.1002/1873-3468.12321.

Characterization of molecular interactions between *E. coli* RNA polymerase and topoisomerase I by molecular simulations

Purushottam Babu Tiwari^{1,*}, Prem P. Chapagain^{2,3}, Srikanth Banda^{3,4}, Yesim Darici², Aykut Üren¹, and Yuk-Ching Tse-Dinh^{3,4,*}

¹Department of Oncology, Georgetown University, Washington, District of Columbia

²Department of Physics, Florida International University, Miami, Florida

³Biomolecular Sciences Institute, Florida International University, Miami, Florida

⁴Department of Chemistry and Biochemistry, Florida International University, Miami, Florida

Abstract

Escherichia coli topoisomerase I (EctopI), a type IA DNA topoisomerase, relaxes the negative DNA supercoiling generated by RNA polymerase (RNAP) during transcription elongation. Due to the lack of structural information on the complex, the exact nature of the RNAP-EctopI interactions remains unresolved. Herein, we report for the first time, the structure-based modeling of the RNAP-EctopI interactions using computational methods. Our results predict that the salt-bridge as well as hydrogen bond interactions are responsible for the formation and stabilization of the RNAP-EctopI complex. Our investigations provide molecular insights for understanding how EctopI interacts with RNAP, a critical step for preventing hypernegative DNA supercoiling during transcription.

Keywords

MD simulations; RNA polymerase; *E. coli* topoisomerase I; salt-bridge; hydrogen bonds; SPR

Introduction

DNA-dependent RNA polymerase (RNAP) performs transcription in all organisms and this involves initiation, elongation, and termination stages [1–4]. RNAP core subunits are highly homologous in both prokaryotes and eukaryotes [5–7]. During transcription, RNAP leaves behind transcription driven negative supercoiling in DNA and creates a positive supercoiling

*Corresponding Authors: Purushottam B. Tiwari, pbt7@georgetown.edu, Phone: +1(202) 687-8478, Fax: +1 (202) 687-1434, Yuk-Ching Tse-Dinh, ytsedinh@fiu.edu, Phone: +1(305) 348-4956, Fax: +1 (305) 348-3772.

Supporting information

SPR experimental and MD simulation procedures, RMSD and RMSF measurements, and movie showing the dynamics of the RNAP-EctopI complex is available at <http://febs.onlinelibrary.wiley.com/xxxxxxxxxxxxxx>.

Author contributions

P. B. T. and Y. T. designed the overall research project. P. B. T. performed molecular docking, MD simulation, and SPR experiment. P. B. T. and P. C. designed the MD simulations and analyzed the simulation data. S. B. purified EctopI for SPR experiment and performed sequence alignments. P. B. T., Y. D., A. U. and Y. T. contributed to SPR experimental design and data analysis. P. B. T. wrote and P. C. and Y. T. edited the manuscript. S. B., Y. D. and A. Ü. also contributed to manuscript editing.

tension ahead of RNAP complex as it progresses forward [8–10]. Such supercoiling tension must be relieved by DNA topoisomerases [11].

DNA topoisomerases play crucial role in many cellular processes, including transcription. Bacterial type IA DNA topoisomerases relax negative supercoils in DNA [12]. *Escherichia coli* topoisomerase I (EctopoI) is the most extensively studied bacterial type IA topoisomerase, consisting of 865 amino acids residues. The active site residue Y319 establishes a transient covalent linkage with the 5' phosphoryl group of a cleaved single strand DNA during its catalytic action [13]. The lack of EctopoI activity leads to R-loop formation and suppression of the transcription elongation [14,15]. Based on a hypothesis of the possibility of direct protein-protein interactions between RNAP and EctopoI, a previous experimental investigation found that the RNAP β' subunit interacts with the C-terminal domain (CTD) of EctopoI (EctopoI-CTD), establishing an inter-protein complex between RNAP and EctopoI [16]. However, due to the lack of structural information on the complex including identification of the key residues for the complex formation, the exact nature of the RNAP-EctopoI interactions is not well understood. Herein, we report the in-silico docking and molecular dynamics (MD) results for the modeling of the RNAP-EctopoI complex and site-specific binding of RNAP to EctopoI. Molecular docking studies have been used to predict protein-protein complexes [17,18] and binding interface [19]. The strength of interactions between proteins can be quantified through the determination of the equilibrium dissociation constant (K_D), also known as the binding affinity [20]. We performed surface plasmon resonance (SPR) based experiments [21–24] to determine the K_D value of RNAP and EctopoI interaction. As flexible macromolecules, the structure and function of proteins are related to their conformational dynamics [25] and computational investigations can provide information on how conformational flexibility accommodates its binding partner as well as the stability of the complex after binding [26]. MD simulations can be used to investigate complex formation between a protein and its binding partners [27]. In order to model the structural features of RNAP binding to EctopoI, we performed all-atom MD simulations for the RNAP-EctopoI complex predicted by molecular docking.

The RNAP-EctopoI complex is predicted by molecular docking to establish through interactions between the RNAP β' subunit and the C-terminal domain (CTD) of EctopoI, in agreement with previous experimental results [16]. The interactions between the RNAP β' subunit and EctopoI-CTD were further investigated by all-atom MD simulations. The complex was found to be stable for the entire 150 ns of simulation. Our results show that EctopoI latches on to the RNAP β' subunit through two hydrogen bonds formed by S1117 (RNAP) with K664 (EctopoI), and V967 (RNAP) with K664 (EctopoI). These interactions were found to be highly stable throughout the simulation. Moreover, a significant structural rearrangement was observed in the RNAP β' subunit as the complex establishes further inter-protein interactions, including the two salt-bridges E874 (RNAP)-K627 (EctopoI) and E1009 (RNAP)-K609 (EctopoI). We propose that the hydrogen bonds initiate the complex formation and allow the significant structural flexibility and reorganization in RNAP without breaking the complex.

Materials and methods

Molecular docking

The structure of the *E. coli* RNAP core enzyme was taken from protein data bank (PDB) [PDB entry 3LU0 [28]]. Protein coordinates in the PDB entry 4RUL [29] was taken as the full-length structure of EctopI. Molecular docking between these two proteins was performed using the PatchDock web server [30,31]. The top 100 predictions from the PatchDock docked complexes were refined using FireDock web server [32,33]. The best-ranked complex with the lowest energy (highest affinity) from the FireDock output was considered as the RNAP-EctopI complex for further analysis.

Surface plasmon resonance (SPR)

Biacore T200 SPR instrument was used to determine the K_D value for RNAP-EctopI complex formation. More detailed information about SPR experiment is given in the Supporting information (Section S1).

Molecular dynamics (MD) Simulations

All-atom MD simulations were carried out with the NAMD simulation package [34]. The input files/parameters for MD simulations were generated by CHARMM-GUI [35] using CHARMM36 force field. Further details about MD simulation methods can be found in the Supporting information (Section S2).

Data analysis

Biaevaluation software version 2.0 was used to evaluate the SPR sensorgrams in order to determine K_D value via steady state affinity analysis. Each frame in the simulation trajectory file was saved at every 20 ps. VMD [36] was used to visualize the structure and analyze the simulation trajectories.

Results and discussion

The structure of the most favorable RNAP-EctopI complex, predicted by PatchDock and refined by FireDock (see Materials and methods section above) is displayed in Fig. 1A. Fig. 1B represents the cartoon structure of the RNAP-EctopI complex selected for MD simulations. The binding interface of the complex shows that the RNAP β' subunit and the EctopI-CTD are involved in establishing the complex between RNAP and EctopI. This result is consistent with previous experimental evidence suggesting that the complex between these two proteins is formed between the RNAP β' subunit and EctopI-CTD [16]. We quantitatively characterized this complex (RNAP-EctopI) formation by determining the equilibrium dissociation constant (K_D) using SPR technique. The steady state response values (shown by the shaded grey area in Fig. 1C) were plotted vs. the RNAP concentration as shown in Fig. 1D and were evaluated using Biaevaluation software version 2.0 via steady state affinity model fitting. A K_D value of ~93 nM was obtained for the RNAP-EctopI protein-protein interaction.

Analysis of the RNAP-EctopoI complex interface (Fig. 1E) after the energy minimization shows that several hydrogen bond, ionic, and van der Waals interactions are involved in forming and stabilizing the RNAP-EctopoI complex. The interfacial contacts involve mainly the residues in the EctopoI loop segments that are stabilized by Zn^{2+} co-ordinations at the two ends. Specifically, inter-protein salt-bridge interactions between E873 (RNAP) and K627 (EctopoI), and between K959 (RNAP) and E628 (EctopoI) occur at the interface involving one of the Zn^{2+} bound loop of the EctopoI-CTD. Other specific interactions include hydrogen bond between S876 (RNAP) and E628 (EctopoI), and between V967 (RNAP, backbone) and K664 (EctopoI, side chain). Although these salt-bridge and hydrogen-bond interaction pairs change during the MD simulation as discussed later, the residues involved in such interactions represent the recognition sites for EctopoI-CTD binding to RNAP. Remarkably, the EctopoI region that binds to RNAP is very close to the location where it binds the single stranded DNA in the crystal structure of the EctopoI-DNA complex, making the inter-protein interactions in this region functionally relevant, as the CTD may be interacting with one of the unwound DNA strands upon its exit from the RNAP transcription elongation complex. Fig. 1F shows the ssDNA-bound EctopoI structure (PDB ID: 4RUL).

In order to assess the stability and to optimize the conformational integrity of the docked complex, we performed all-atom MD simulations in explicit solvent. The dynamics incorporates residue flexibility and allows proteins to undergo structural adjustments for improving interfacial contacts. Being a fairly large system, detailed all-atom simulations of the full complex is computationally costly. The RNAP β' subunit alone consists of ~1400 amino acid residues. Therefore, for the MD simulations we selected only the domains that are involved in the inter-protein interactions as shown in Fig. 1B. The regions of the complex selected for the MD simulations consisted of residues 594–705 of EctopoI and residues 788–1317 of the RNAP β' subunit. The stability of proteins structures were confirmed by measuring the root mean square deviations (RMSD) of backbone atoms and root-mean-square fluctuations (RMSF) for the C_{α} atoms (Supporting information, Section S3).

We monitored the interfacial contacts of the complex during the MD simulations. Interestingly, a significant rearrangement of the interfacial contacts was observed. Fig. 2A shows the final structure the complex at the end of the 150 ns NVT simulation. Important interfacial amino acid residues that stabilize the complex are highlighted. These contacts are observed in three different sites, two of which still involve residues in the loop segments that are stabilized by the Zn^{2+} co-ordinations at the two ends of EctopoI. Relatively more stable interfacial contacts are made in the Zn^{2+} coordinated loop involving K664. Specifically, the positively charged K664 (EctopoI) side chain forms two hydrogen bonds: with the S1117 side chain and the V967 backbone (RNAP β' subunit).

The amino acid residues in EctopoI that establish salt-bridges with RNAP are generally conserved among various bacterial species, as shown in Fig. 2C. Interestingly, when lysine in position 664 is replaced by isoleucine, its binding counterpart serine in position 1117 is also replaced by isoleucine or valine. This makes it possible for these residues to interact via hydrophobic interactions. Slight structural rearrangements yield two new salt-bridges K627

(EctopoI)-E874 (RNAP) and R609 (EctopoI)-E1009 (RNAP) to replace the two originally observed ionic interactions K627 (EctopoI)-E873 (RNAP) and E628 (EctopoI)-K959 (RNAP). The salt-bridge interaction between R609 (EctopoI) and E1009 (RNAP) occurs about midway between the Zn^{2+} co-ordinated sites. Fig. 2B shows the time evolution of the distances between the residue-pairs involved in specific interactions at the interface of the final structure of the complex. The two new salt-bridge interactions form only after 30 ns. Once formed, the E1009-R609 salt-bridge in the middle is quite stable, whereas the E874-K627 salt-bridge forms and breaks intermittently due to structural fluctuations of the RNAP β' subunit as discussed later. The hydrogen bonds involving K664 are very stable throughout the trajectory. The Zn^{2+} ion in the loop containing K664 gives structural support for the loop. These observations suggest that the EctopoI-CTD first latches on to RNAP β' subunit through the loop containing K664 and the strong inter-protein interactions in this region allow structural flexibility and reorganization in RNAP without breaking the complex.

Protein-protein interactions exhibit dynamic structural reorganizations of the binding partners [23]. It is worth noting that the RNAP β' subunit displays interesting conformational changes during the complex formation and stabilization, whereas the conformation of EctopoI remains relatively stable (see movie in the Supporting Information, Section S4). Once the EctopoI-CTD latches on to the RNAP β' subunit, the domain fluctuation exposes E874 that is originally buried between the domains and facilitates further interactions between EctopoI and RNAP. Fig. 3 displays various stages of the structural changes. Fig. 3A shows the complex structure at the beginning of the NVT simulation (0 ns). The dotted circle represents the RNAP region that undergoes significant structural changes. Between 0–25 ns, the circled RNAP region expands slightly, which allows the buried E874 to expose (Fig. 3B) and make itself available for interacting with EctopoI. This structural change corresponds to the RMSD fluctuations between 0–25 ns as shown (Supporting information, Section S3). After ~30 ns, an inter-protein salt-bridge is formed between E874 and K627, as shown in Fig. 3C (at ~45 ns). This salt-bridge, however, is transiently stable as the two sub-domains of the RNAP β' subunit continue to fluctuate. Fig. 3D at 65 ns shows a broken salt bridges, whereas Fig. 3E (at 80 ns) and Fig. 3F (at 120 ns) intact salt-bridges. This behavior is also displayed in Fig. S1A (red curve, Supporting information,). Further structural adjustments (>150 ns) will likely stabilize this interaction and enhance the structural integrity of the RNAP-EctopoI complex.

To further investigate the role of the hydrogen bonds between K664 side chain and V667 backbone as well as S1117 side chain on stabilizing the complex, we performed additional MD simulations for the complex with K664A substitution in EctopoI. Simulations were run under the same conditions as for the wild-type (WT) RNAP-EctopoI complex. The mutant RNAP-EctopoI complex (Fig. 4A) was dissociated by 45 ns (Fig. 4B) of the simulation, conforming the critical role played by the interfacial residues K664, V967 and S1117 in the initiation and stabilization of the complex. Interestingly, as EctopoI interacts with RNAP, the RNAP β' subunit is observed to undergo similar structural fluctuations as seen in the WT complex.

Conclusions

We investigated the formation and stabilization of the RNAP-EctopoI complex using MD simulations. Consistent with a previous experimental result, the predicted binding interface using molecular docking involves the RNAP β' subunit and the EctopoI-CTD. The complex was stable throughout the 150 ns of MD simulation. Our results show that the two salt-bridges between E874 (RNAP) and K627 (EctopoI), and E1009 (RNAP) and R609 (EctopoI) as well as two hydrogen bonds between S1117 (RNAP) and K664 (EctopoI), and V967 (RNAP) and K664 (EctopoI) comprise the major interfacial interactions in the RNAP-EctopoI complex. Upon EctopoI binding, RNAP was found to undergo conformational rearrangements, facilitating the inter-protein interactions. The mutant complex with the K664A substitution is found to be unstable. The removal of the specific interactions involving K664 and S1117 allows the complex to dissociate, with no inter-protein contacts left by 45 ns of simulation. Based on these observations, we propose that the EctopoI loop containing K664 is responsible for the initiation of the complex formation. Since this loop is stabilized by Zn^{2+} co-ordination, the results suggest that the Zn^{2+} co-ordination might also be important for the complex formation. Our very first structural characterization of the RNAP-EctopoI complex provides insights on EctopoI binding to RNAP, a critical step for relaxing hypernegative DNA supercoiling during transcription, and opens the door for further investigations on protein-protein or protein-DNA interactions in this important system.

Supplementary Material

Refer to Web version on PubMed Central for supplementary material.

Acknowledgments

This work is supported by National Institutes of Health (NIH) grants R01GM054226 (Y. T.). Experimental SPR sensorgrams were measured by using Biacore T200 instrument available in Biacore Molecular Interaction Shared Resource (BMISR) facility at Georgetown University. The BMISR is supported by NIH grant P30CA51008.

References

1. Ray-Soni A, Bellecourt MJ, Landick R. Mechanisms of Bacterial Transcription Termination: All Good Things Must End. 2016
2. Vassilyev DG, Vassilyeva MN, Perederina A, Tahirov TH, Artsimovitch I. Structural basis for transcription elongation by bacterial RNA polymerase. *Nature*. 2007; 448:157–162. [PubMed: 17581590]
3. Feklistov A. RNA polymerase: in search of promoters. *Ann. N. Y. Acad. Sci.* 2013; 1293:25–32. [PubMed: 23855603]
4. Vassilyev DG. Elongation by RNA polymerase: a race through roadblocks. *Curr. Opin. Struct. Biol.* 2009; 19:691–700. [PubMed: 19896365]
5. Sweetser D, Nonet M, Young RA. Prokaryotic and Eukaryotic RNA Polymerases Have Homologous Core Subunits. *Proc. Natl. Acad. Sci. U. S. A.* 1987; 84:1192–1196. [PubMed: 3547406]
6. Cramer P. Multisubunit RNA polymerases. *Curr. Opin. Struct. Biol.* 2002; 12:89–97. [PubMed: 11839495]
7. Ebricht RH. RNA Polymerase: Structural Similarities Between Bacterial RNA Polymerase and Eukaryotic RNA Polymerase II. *J. Mol. Biol.* 2000; 304:687–698. [PubMed: 11124018]

8. Vos SM, Tretter EM, Schmidt BH, Berger JM. All tangled up: how cells direct, manage and exploit topoisomerase function. *Nat. Rev. Mol. Cell Biol.* 2011; 12:827–841. [PubMed: 22108601]
9. Liu LF, Wang JC. Supercoiling of the DNA template during transcription. *Proc. Natl. Acad. Sci. U. S. A.* 1987; 84:7024–7027. [PubMed: 2823250]
10. Ma J, Bai L, Wang MD. Transcription under torsion. *Science.* 2013; 340:1580–1583. [PubMed: 23812716]
11. Wu HY, Shyy SH, Wang JC, Liu LF. Transcription generates positively and negatively supercoiled domains in the template. *Cell.* 1988; 53:433–440. [PubMed: 2835168]
12. Champoux JJ. DNA topoisomerases: structure, function, and mechanism. *Annu. Rev. Biochem.* 2001; 70:369–413. [PubMed: 11395412]
13. Lynn RM, Wang JC. Peptide sequencing and site-directed mutagenesis identify tyrosine-319 as the active site tyrosine of *Escherichia coli* DNA topoisomerase I. *Proteins.* 1989; 6:231–239. [PubMed: 2560190]
14. Drolet M, Phoenix P, Menzel R, Masse E, Liu LF, Crouch RJ. Overexpression of RNase H partially complements the growth defect of an *Escherichia coli* delta topA mutant: R-loop formation is a major problem in the absence of DNA topoisomerase I. *Proc. Natl. Acad. Sci. U. S. A.* 1995; 92:3526–3530. [PubMed: 7536935]
15. Massé E, Drolet M. *Escherichia coli* DNA Topoisomerase I Inhibits R-loop Formation by Relaxing Transcription-induced Negative Supercoiling. *J. Biol. Chem.* 1999; 274:16659–16664. [PubMed: 10347234]
16. Cheng B, Zhu C-X, Ji C, Ahumada A, Tse-Dinh Y-C. Direct Interaction between *Escherichia coli* RNA Polymerase and the Zinc Ribbon Domains of DNA Topoisomerase I. *J. Biol. Chem.* 2003; 278:30705–30710. [PubMed: 12788950]
17. Smith GR, Sternberg MJ. Prediction of protein-protein interactions by docking methods. *Curr. Opin. Struct. Biol.* 2002; 12:28–35. [PubMed: 11839486]
18. Gray JJ, Moughon S, Wang C, Schueler-Furman O, Kuhlman B, Rohl CA, Baker D. Protein-protein docking with simultaneous optimization of rigid-body displacement and side-chain conformations. *J. Mol. Biol.* 2003; 331:281–299. [PubMed: 12875852]
19. Xue LC, Dobbs D, Bonvin AMJJ, Honavar V. Computational prediction of protein interfaces: A review of data driven methods. *FEBS Lett.* 2015; 589:3516–3526. [PubMed: 26460190]
20. Kastiris PL, Bonvin AMJJ. On the binding affinity of macromolecular interactions: daring to ask why proteins interact. *J. R. Soc. Interf.* 2013; 10 20120835.
21. Tiwari PB, Annamalai T, Cheng B, Narula G, Wang X, Tse-Dinh YC, He J, Darici Y. A surface plasmon resonance study of the intermolecular interaction between *Escherichia coli* topoisomerase I and pBAD/Thio supercoiled plasmid DNA. *Biochem. Biophys. Res. Commun.* 2014; 445:445–450. [PubMed: 24530905]
22. Ellass E, Coddeville B, Guéardel Y, Kremer L, Maes E, Mazurier J, Légrand D. Identification by surface plasmon resonance of the mycobacterial lipomannan and lipoarabinomannan domains involved in binding to CD14 and LPS-binding protein. *FEBS Lett.* 2007; 581:1383–1390. [PubMed: 17350002]
23. Tiwari PB, et al. Characterization of molecular mechanism of neuroglobin binding to cytochrome c: A surface plasmon resonance and isothermal titration calorimetry study. *Inorg. Chem. Commun.* 2015; 62:37–41.
24. Banda S, Tiwari PB, Darici Y, Tse-Dinh YC. Investigating direct interaction between *Escherichia coli* topoisomerase I and RecA. *Gene.* 2016; 585:65–70. [PubMed: 27001450]
25. Karplus M, McCammon JA. Molecular dynamics simulations of biomolecules. *Nat. Struct. Mol. Biol.* 2002; 9:646–652.
26. Singh W, Karabencheva-Christova TG, Black GW, Ainsley J, Dover L, Christov CZ. Conformational Dynamics, Ligand Binding and Effects of Mutations in NirE an S-Adenosyl-L-Methionine Dependent Methyltransferase. *Sci. Rep.* 2016; 6:20107. [PubMed: 26822701]
27. Shvetsov AV, et al. Structure of RecX protein complex with the presynaptic RecA filament: Molecular dynamics simulations and small angle neutron scattering. *FEBS Lett.* 2014; 588:948–955. [PubMed: 24530684]

28. Opalka N, Brown J, Lane WJ, Twist K-AF, Landick R, Asturias FJ, Darst SA. Complete Structural Model of *Escherichia coli* RNA Polymerase from a Hybrid Approach. *PLoS Biol.* 2010; 8:e1000483. [PubMed: 20856905]
29. Tan K, Zhou Q, Cheng B, Zhang Z, Joachimiak A, Tse-Dinh Y-C. Structural basis for suppression of hypernegative DNA supercoiling by *E. coli* topoisomerase I. *Nucleic Acids Res.* 2015; 43:11031–11046. [PubMed: 26490962]
30. Duhovny, D.; Nussinov, R.; Wolfson, HJ. Efficient Unbound Docking of Rigid Molecules. In: Guigó, R.; Gusfield, D., editors. *Algorithms in Bioinformatics: Second International Workshop, WABI 2002 Rome, Italy, September 17–21, 2002 Proceedings.* Berlin: Springer Verlag Berlin; p. 185-200.
31. Schneidman-Duhovny D, Inbar Y, Nussinov R, Wolfson HJ. PatchDock and SymmDock: servers for rigid and symmetric docking. *Nucleic Acids Res.* 2005; 33:W363–W367. [PubMed: 15980490]
32. Mashiach E, Schneidman-Duhovny D, Andrusier N, Nussinov R, Wolfson HJ. FireDock: a web server for fast interaction refinement in molecular docking. *Nucleic Acids Res.* 2008; 36:W229–W232. [PubMed: 18424796]
33. Andrusier N, Nussinov R, Wolfson HJ. FireDock: Fast interaction refinement in molecular docking. *Proteins: Struct. Funct. Bioinf.* 2007; 69:139–159.
34. Phillips JC, et al. Scalable molecular dynamics with NAMD. *J. Comput. Chem.* 2005; 26:1781–1802. [PubMed: 16222654]
35. Lee J, et al. CHARMM-GUI Input Generator for NAMD, GROMACS, AMBER, OpenMM, and CHARMM/OpenMM Simulations Using the CHARMM36 Additive Force Field. *J. Chem. Theory . Comput.* 2016; 12:405–413. [PubMed: 26631602]
36. Humphrey W, Dalke A, Schulten K. VMD: Visual molecular dynamics. *J. Mol. Graphics.* 1996; 14:33–38.

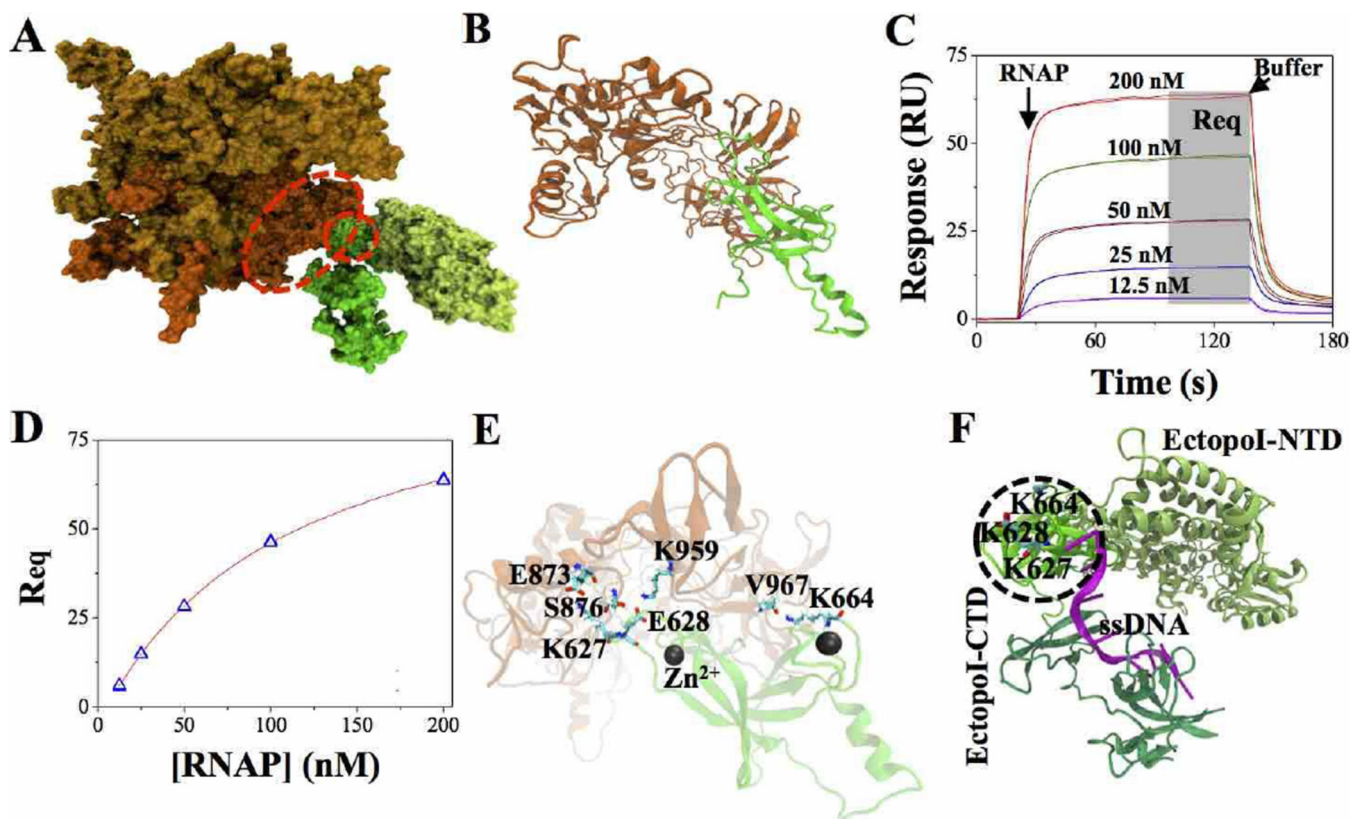


Fig. 1. RNAP-EctopoI complex formation. (A) The most favorable complex, in surface representation, as predicted by docking. Orange and gold colored structure represents RNAP (orange: RNAP β' subunit). Green colored structure represents EctopoI (dark green: EctopoI-CTD and light green: EctopoI-NTD). The structures inside the red dotted curve depict portions of the RNAP β' subunit and EctopoI-CTD considered for MD simulations. (B) Cartoon structure of the RNAP-EctopoI complex selected for MD simulations. (C) SPR sensorgrams for RNAP (analyte), at various concentrations (in duplicates), binding to immobilized EctopoI (ligand) on the CM5 sensor chip. The arrows show the start of analyte and buffer injections. (D) Steady state response values (Req, gray shaded area in Fig. 1C) plotted as a function of RNAP concentrations. The continuous line represents the steady state affinity fit using Biaevaluation software version 2.0. (E) Cartoon structure of the RNAP-EctopoI complex, showing the interfacial residues in contact after energy minimization. (F) EctopoI-ssDNA bound structure (PDB ID: 4RUL) (green: EctopoI-CTD portion selected for simulation; magenta: ssDNA bound to EctopoI-CTD) The bases of the DNA in the RNAP interacting region are held in position through pi-stacking with F616 and Y622.

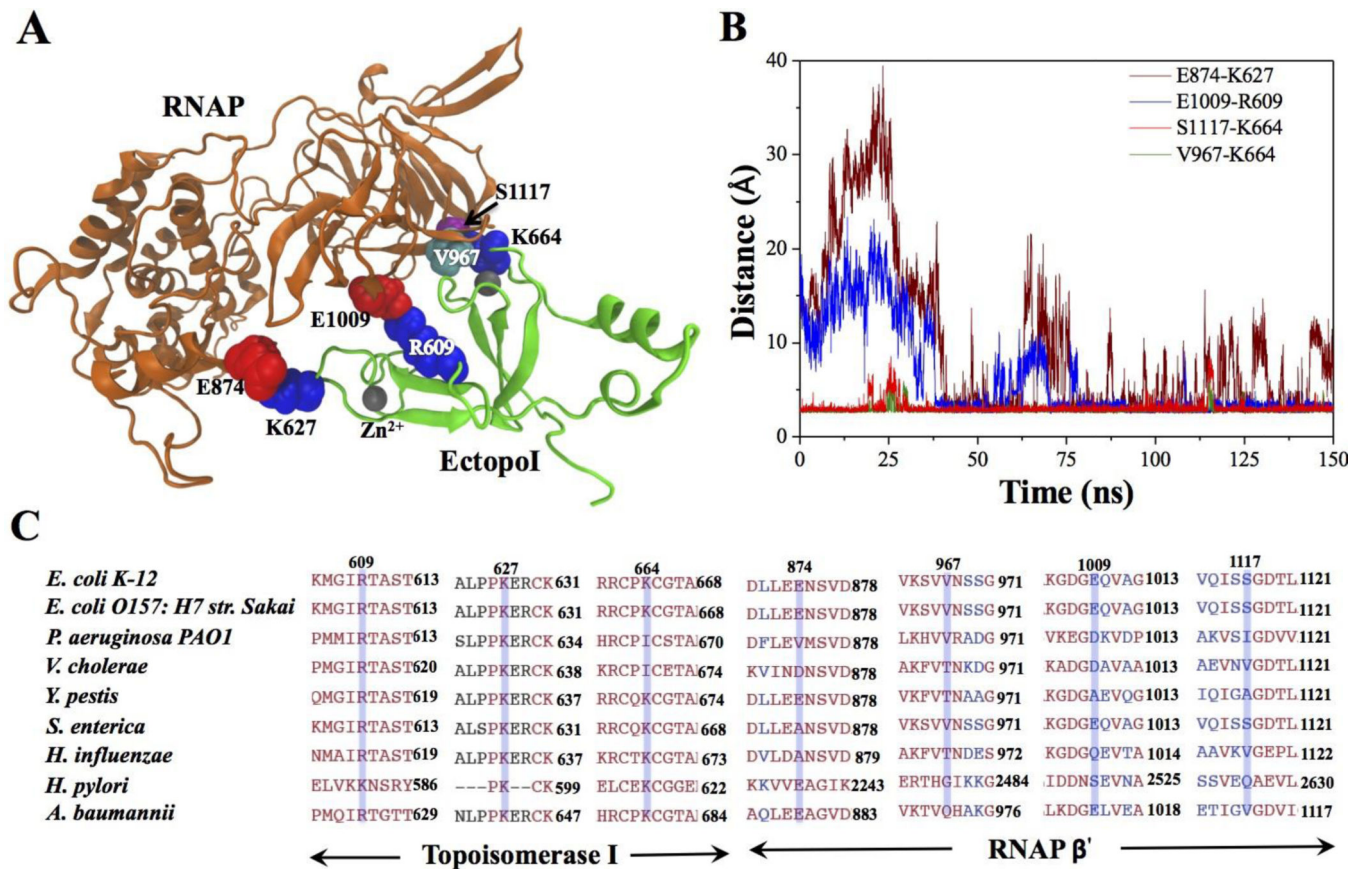


Fig. 2. Interactions between RNAP and Ectopoi across the binding interface. (A) RNAP-Ectopoi complex after 150 ns of NVT simulations (highlighted residues - blue: lysine (K) and arginine (R); red: glutamic acid (E); cyan: valine (V); and purple: serine (S)). (B) Distance between the predicted amino acid residues, over 150 ns trajectory, that form interprotein complex between RNAP and Ectopoi. Each frame in 150 ns of trajectory was recorded at every 20 ps. (C) Sequence alignment of the RNAP β' and Ectopoi for various bacterial species. Blue transparent boxes represent the interfacial residues involved in salt-bridges and hydrogen bonding.

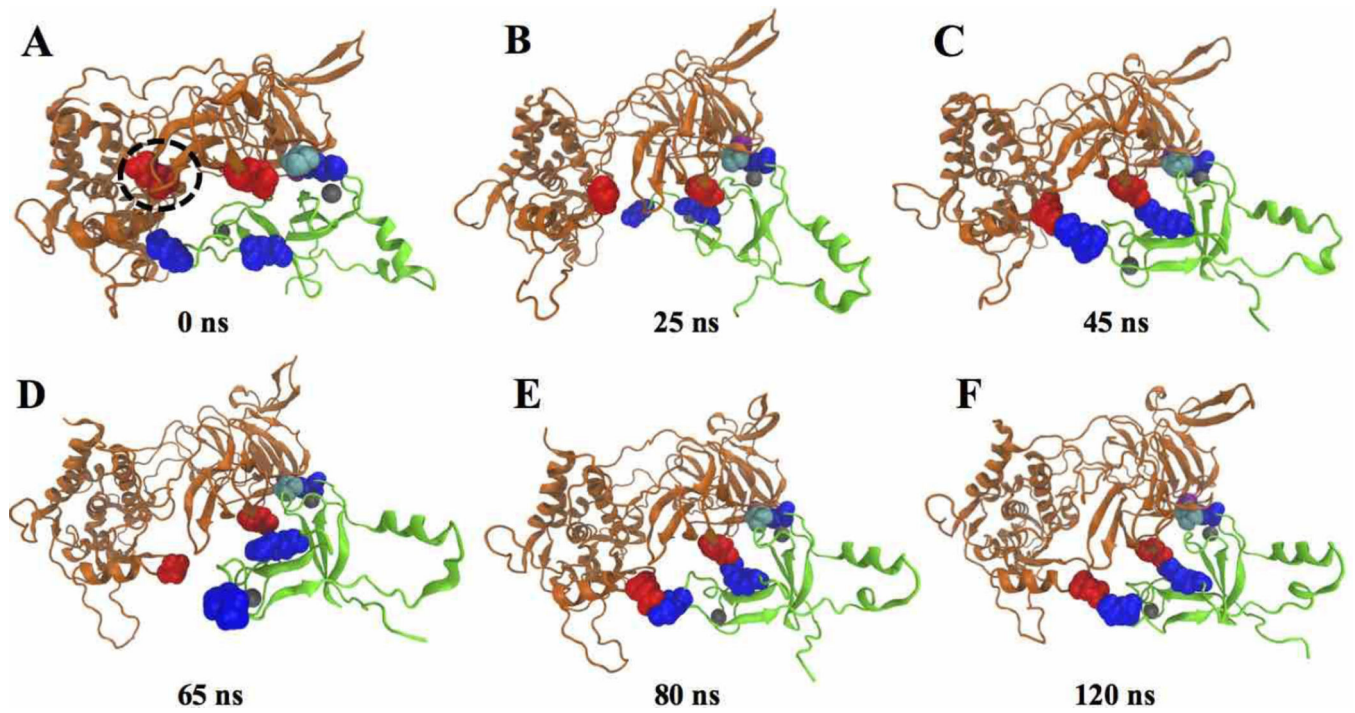


Fig. 3. Structures of the RNAP-EctopI complexes at different times during the simulation trajectory. The structure at (A) 0 ns (starting structure), (B) 25 ns, (C) 45 ns, (D) 65 ns, (E) 80 ns, and (F) 120 ns.

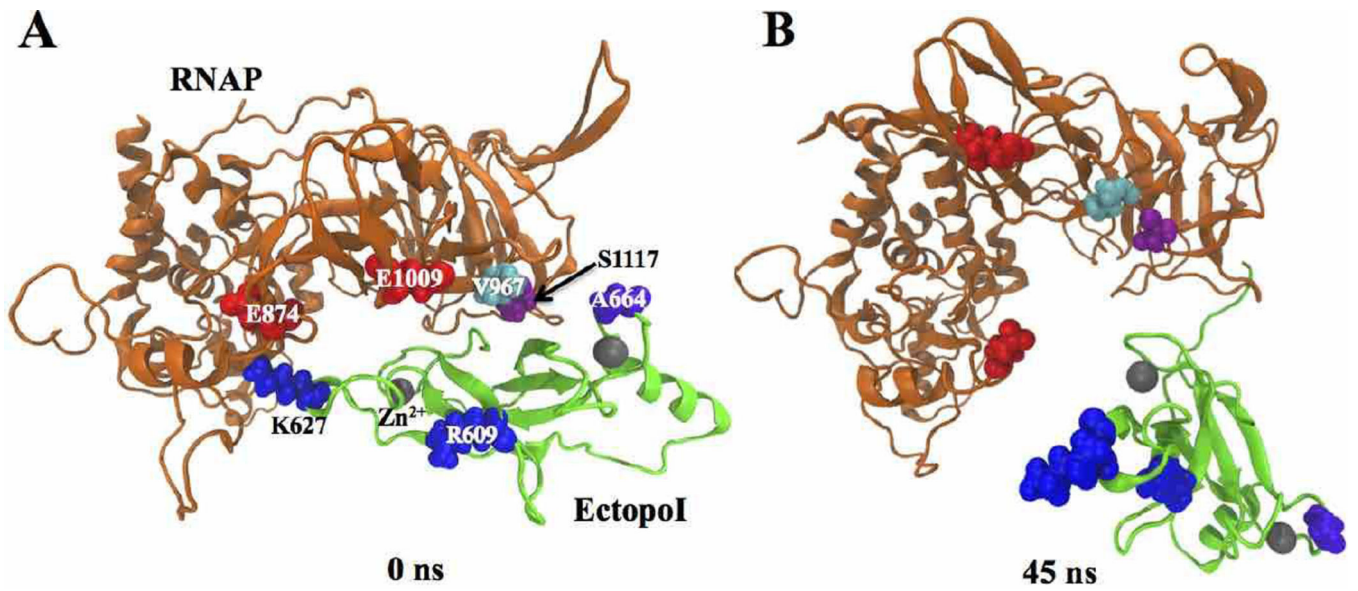


Fig. 4. Mutant RNAP-Ectopoli complexes (with K664A mutation) at different times of the NVT simulation trajectory. Structure of the complex at (A) 0 ns (starting structure) and (B) at 45 ns of the NVT simulations.